Multiple communication mechanisms between sensor kinases are crucial for virulence in *Pseudomonas aeruginosa*

Vanessa I. Francis[1], Elaine M. Waters[2], Sutharsan E. Finton-James[1], Andrea Gori[1], Aras Kadioglu[2], Alan R. Brown[1], Steven L. Porter[1*]

[1]Biosciences, Geoffrey Pope Building, College of Life and Environmental Sciences, University of Exeter, Exeter, EX4 4QD, UK.

[2]Department of Clinical Infection, Microbiology and Immunology, Institute of Infection and Global Health, University of Liverpool, Liverpool, L69 7BE, UK.

***** For correspondence: Dr Steven Porter
Biosciences
Geoffrey Pope Building
College of Life and Environmental Sciences
University of Exeter
Exeter
EX4 4QD
UK
Email: s.porter@exeter.ac.uk
Telephone: +44 1392 722172

ABSTRACT

Bacteria and many non-metazoan Eukaryotes respond to stresses and threats using two-component systems (TCSs) comprising sensor kinases (SKs) and response regulators (RRs). Multikinase networks, where multiple SKs work together, detect and integrate different signals to control important lifestyle decisions such as sporulation and virulence. Here, we study interactions between two SKs from *Pseudomonas aeruginosa*, GacS and RetS, which control the switch between acute and chronic virulence. We demonstrate three mechanisms by which RetS attenuates GacS signalling: RetS takes phosphoryl groups from GacS-P; RetS has transmitter phosphatase activity against the receiver domain of GacS-P; and RetS inhibits GacS autophosphorylation. These mechanisms play important roles *in vivo* and during infection, and exemplify an unprecedented degree of signal processing by SKs that may be exploited in other multikinase networks.

INTRODUCTION

Canonical TCSs, comprising a single SK working with its cognate RR[1,2], detect and respond to stimuli but are not well suited to making complex decisions requiring the integration of multiple signals. However, multikinase-networks, where several SKs collaborate to detect and integrate signals, can make these sophisticated decisions requiring the evaluation of multiple stimuli. Multikinase networks regulate processes as diverse as asymmetric cell division[3-5], sporulation[6], chemotaxis[7], nitrogen metabolism[8], stress responses[9], virulence[10,11], biofilm formation[12], and differentiation into fruiting bodies[13,14]. Many multikinase networks feature interactions between their constituent SKs but how they affect signalling output is unclear[15-17].

Most SKs are homodimeric proteins, containing sensory domains for detecting stimuli and controlling the activity of their catalytic core, comprising the HisKA and HATPase domains. The HATPase domain binds ATP and phosphorylates a histidine residue within the HisKA domain. For simple SKs, following autophosphorylation, phosphotransfer occurs to an aspartate in the receiver (REC) domain of the RR. In more complex SKs (~20% of bacterial and ~90% of eukaryotic examples), additional phosphorylation sites, contained within either attached REC (hybrid SKs) or attached REC and Hpt domains (unorthodox SKs)[18], participate in multi-step phosphorelays, which comprise His-to-Asp and Asp-to-His phosphotransfer reactions, conveying phosphoryl groups to the RR. Phosphorylation activates the RR, mediating a response to the stimulus[19]. Signals are terminated by hydrolysis of the aspartyl-phosphate residue, which is an autocatalytic process, often augmented by either transmitter phosphatase activity of the SK or extrinsic phosphatases[20-22]. The phosphotransfer and phosphatase reactions are highly specific, ensuring fidelity of signalling[23-29].

Pseudomonas aeruginosa is a leading cause of healthcare-acquired-infections[30,31]. It infects vulnerable patients e.g. neonates or those with cystic fibrosis, burn wounds or cancer. It causes acute and chronic infections[32]; acute infections (e.g. pneumonia and sepsis) feature motility and type III secretion (T3S), while, chronic infections (e.g. cystic fibrosis lung) involve biofilm production and type VI secretion (T6S)[32-34]. The GacS multikinase-network plays a key role in orchestrating the transition between acute and chronic infection[35-38]. Central to this network is the unorthodox SK, GacS, which phosphorylates the RR, GacA. GacA-P activates transcription of the regulatory RNAs, RsmY & RsmZ, which sequester the translational regulator, RsmA, thereby upregulating genes required for chronic infection and downregulating acute infection[39-43].

Although only GacS-P phosphorylates GacA, other SKs influence GacA-P levels via GacS. LadS senses calcium[44], and promotes chronic infection by phosphorylating GacS[45,46]. In contrast, the hybrid SK, RetS, binds and inhibits GacS via unknown mechanisms, favouring acute infection[10,47-49]. The ligand controlling RetS is unknown, but RetS responds to lysis of kin *P. aeruginosa* cells[50]. Another SK, PA1611, sequesters RetS, relieving GacS from its inhibition[51,52].

The inhibitory interaction of RetS with GacS is considered the paradigm for negative regulation in multikinase-networks[10]. Previously, it was proposed that they form an inactive heterodimer incapable of autophosphorylation[10]. Here, we demonstrate the interactions are much more extensive, with RetS having three distinct mechanisms for downregulating GacS. All are important for RetS function and play major roles in virulence. These mechanisms represent an unprecedented level of cross-communication between SKs that can be widely utilised by other multikinase-networks.

Results

RetS takes phosphoryl groups from GacS-P in mechanism 1. RetS has a degenerate HATPase domain lacking the conserved G-boxes and consequently is unable to autophosphorylate. The cytoplasmic portions of GacS and RetS (denoted GacSc and RetSc) interact, and the inclusion of RetSc in GacSc autophosphorylation reactions reduces the steady-state levels of GacSc-P produced[10]; here, we determine the molecular mechanisms responsible. We began by testing whether RetSc could accelerate the dephosphorylation of purified GacSc-P (Fig. 1a,b); these reactions did not contain any residual ATP. We detected phosphorylation of RetSc (Fig. 1b), indicating phosphotransfer had occurred from GacSc-P to RetSc. To determine which of the three phosphorylation sites of RetS accepts the phosphoryl group from GacS-P, we prepared mutant RetSc proteins lacking these sites (wild-type RetSc, with its three native phosphorylation sites is denoted RetSc(HDD)). The mutant protein lacking the phosphorylation site in REC1 (D713) was unchanged in its ability to be phosphorylated by GacSc-P (Supplementary Fig. 1). We found that the mutant proteins lacking the phosphorylation site in REC2 (D858), RetSc(HDA) and RetSc(HAA), were not phosphorylated by GacSc-P (Fig. 1c,d), indicating that D858 is phosphorylated by GacSc-P.

To identify which of the three phosphorylation sites of GacSc-P was the phosphodonor for this phosphotransfer reaction, we engineered a mutant GacSc protein, GacSc(HAQ), retaining only its autophosphorylation site and lacking its REC and Hpt domain phosphorylation sites. We found that when purified GacSc(HAQ)-P was coincubated with RetSc, RetSc-P was produced and the intensity of the GacSc(HAQ)-P band was decreased, meaning that phosphotransfer had occurred

from GacSc(HAQ)-P to RetSc (Fig. 1f). RetSc-P levels did not rise to the same extent as GacSc(HAQ)-P levels decreased during this phosphotransfer reaction because RetSc-P dephosphorylates and therefore RetSc-P levels are determined not only by the rate of phosphotransfer from GacSc(HAQ)-P but also by how quickly RetSc-P dephosphorylates. No phosphotransfer was seen from GacSc(HAQ)-P to the mutant RetSc proteins lacking D858, RetSc(HDA) and RetSc(HAA) (Fig. 1g,h). These data indicate that the autophosphorylatable His residue in the HisKA domain of GacS is a phosphodonor for D858 in REC2 of RetS. We refer to this as mechanism 1 (Fig. 1i).

RetS is a transmitter phosphatase for GacS-P in mechanism 2. Wild-type GacSc-P autodephosphorylates with a half-time of 25 ± 2 mins (Fig. 1j,k). RetS mutant proteins, RetSc(HDA) (Fig. 1g) and RetSc(HAA) (Fig. 1h), lacking D858, are disabled for mechanism 1 and cannot dephosphorylate GacSc(HAQ)-P. However, they still speed up the dephosphorylation of wild-type GacSc-P (Fig. 1k); each reducing the half-time from 25 ± 2 mins to 15 ± 1 mins (Fig. 1k). Likewise, $RetS_{HK}$, lacking both REC domains and comprising only the catalytic core (HisKA and the degenerate HATPase domain) of RetS, also reduced the GacSc-P dephosphorylation half-time (Fig. 1j,k). This suggests RetS has a second mechanism for dephosphorylating GacS-P that resides within the catalytic core of RetS, and targets either the REC or Hpt phosphorylation sites of GacS (present in wild-type GacSc-P but not in GacSc(HAQ)-P). We examined the dephosphorylation of GacSc(HDQ)-P, which lacks the phosphorylation site in the Hpt domain, and found that RetSc(HDA) and $RetS_{HK}$ could catalyse its dephosphorylation (Supplementary Fig. 2), indicating that the Hpt phosphorylation site is not the target and therefore the target is the REC domain phosphorylation site.

The majority of SKs have kinase and phosphatase activity. While RetS has a degenerate HATPase domain rendering it incapable of autophosphorylation, its HisKA domain retains the conserved H-box including the motif (HExxT) needed for transmitter phosphatase activity[20,53]. We therefore, hypothesised that RetS has transmitter phosphatase activity directed towards the REC domain of GacS. Consistent with this, the mutant protein, RetSc(T428A,HDA), lacking both the conserved T428 residue from the HExxT phosphatase motif, and D858 required for mechanism 1, had no ability to speed up GacSc-P dephosphorylation (Fig. 1k). Therefore, mechanism 2 is enhanced dephosphorylation of GacS-P by transmitter phosphatase activity of RetS against the REC domain of GacS (Fig. 1l).

RetS inhibits the autophosphorylation of GacS in mechanism 3. Mechanisms 1 and 2, described above, dephosphorylate GacS-P. Here we tested whether RetS could affect the autophosphorylation rate of GacS; we did this using mutant versions of GacSc and RetSc where both dephosphorylation mechanisms were disabled. RetSc(HAA) cannot dephosphorylate GacSc(HAQ)-P (Fig. 1h); however, the presence of RetSc(HAA) in a GacSc(HAQ) autophosphorylation reaction, reduced the level of GacSc(HAQ)-P that accumulated (Fig. 1m). Likewise, RetSc(T428A,HDA) which is disabled for mechanisms 1 and 2 (Fig. 1k), inhibited the autophosphorylation of GacSc(HAQ) (Fig. 1m). Similar results were seen when using only the kinase catalytic cores (HisKA and HATPase domain) of GacS and RetS; the presence of $RetS_{HK}$ in a $GacS_{HK}$ autophosphorylation reaction, reduced the level of $GacS_{HK}$-P that accumulated (Fig. 1n). This means there is a third mechanism of interaction between GacS and RetS where the kinase core of RetS inhibits autophosphorylation of GacS (Fig. 1o).

Mechanisms 1 and 2 control biofilm formation. To determine the relative contribution of the three mechanisms *in vivo*, we replaced the wild-type *retS* gene in the chromosome with mutant versions; the *retS*(HDA) mutant lacking mechanism 1, the *retS*(T428A) mutant lacking mechanism 2, the *retS*(T428A,HDA) mutant lacking mechanisms 1 and 2, and the Δ*retS* mutant lacking all three mechanisms. We confirmed that the mutant proteins were expressed at comparable levels to wild-type RetS by western blotting (Supplementary Note 1 and Supplementary Fig. 3).

Deletion of *retS* enhances biofilm formation (Fig. 2)[47,48,54]. The *retS* point mutants (*retS*(HDA), *retS*(T428A) and *retS*(T428A,HDA)) produced significantly more biofilm than the PAO1 strain (Fig. 2a). The mutant lacking mechanism 1, *retS*(HDA), had similar biofilm levels to the Δ*retS* mutant, indicating that mechanism 1 plays a major role in regulating biofilm formation. While biofilm levels were significantly higher in the *retS*(T428A) mutant than in the wild-type strain, they were not elevated to the same extent as the Δ*retS* mutant, indicating that mechanism 2 plays a significant role in controlling biofilm formation although to a lesser extent than mechanism 1. To verify that the increased biofilm formation observed in the *retS* point mutants was a consequence of GacS dysregulation, we introduced these mutations into a Δ*gacS* background. Like their parent Δ*gacS* mutant, these double *gacS*/*retS* mutants produced significantly less biofilm than the PAO1 strain (Supplementary Fig. 4), consistent with the *retS* point mutations affecting signalling via GacS. These data indicate that the control of GacS signalling by mechanisms 1 and 2 of RetS are important for regulating biofilm formation.

Contribution of the three mechanisms to controlling RsmY&Z. The GacS network controls the expression of two small RNAs, RsmY and RsmZ[55]. The Δ*retS* mutant has elevated levels of RsmY and RsmZ because of its increased GacS

activity[10,55,56]. We found that levels of RsmY and RsmZ were increased in all *retS* point mutant strains lacking mechanisms 1 and 2 (Fig. 2b,c), indicating that these mechanisms play major roles in controlling *rsmY* and *rsmZ* expression. The mutant lacking both mechanisms 1 and 2 (*retS*(T428A,HDA)), however, did not produce as much RsmZ as the Δ*retS* mutant (Fig. 2c), suggesting that mechanism 3, alongside mechanisms 1 and 2, contributes a significant role to controlling the expression of *rsmZ.*

Mechanism 1 is important for swarming motility. Unlike the wild-type strain, PAO1, the Δ*retS* mutant did not swarm (Fig. 3). We found that all mutants lacking mechanism 1, e.g. *retS*(HDA) (Fig. 3b) were unable to swarm, indicating that mechanism 1 is essential. The mutant lacking mechanism 2, *retS*(T428A), did swarm, indicating that mechanism 2 is not required (Fig. 3c).

Virulence in *Galleria mellonella* requires mechanisms 1 and 2. To assess the role of the three mechanisms in virulence, the *retS* mutants were tested in a *Galleria mellonella* infection model. Larvae were injected with 20-40 CFUs of PAO1 or mutant strains. The PAO1 infected larvae all died within 21 hours of infection, whereas over 60 % of the larvae infected with the Δ*retS* mutant survived to the end of the experiment (47 hours post-infection) (Fig. 4a). Similar to the Δ*retS* mutant, the *retS*(HDA) and *retS*(T428A,HDA) mutants showed severely attenuated virulence with significantly more larvae surviving than those infected with PAO1 (Fig. 4a). The *retS*(T428A) mutant showed significantly delayed killing compared to those infected with PAO1 (Fig. 4a). We examined the phenotypes of the *retS*(HDA)Δ*gacS* and the *retS*(T428A)Δ*gacS* mutants and found that they were as virulent as the Δ*gacS* mutant (Fig. 4b), confirming that the reduction in virulence seen in the *retS*(HDA) and

208 *retS*(T428A) mutants were dependent on the presence of GacS and therefore a
209 consequence of GacS dysregulation. In summary, mechanism 1 is essential for
210 virulence in *G. mellonella* whereas loss of mechanism 2 delays killing.

211 **RetS overexpression allows mechanism 3 to support virulence.** The mutant
212 lacking mechanisms 1 and 2, *retS*(T428A,HDA), phenocopies the Δ*retS* mutant in
213 most of the above assays, with the only significant difference being that RsmZ levels
214 are not elevated to the same extent as the Δ*retS* mutant (Fig. 2c). This indicates that
215 mechanism 3 alone is not sufficient for RetS function, and that dephosphorylation of
216 GacS-P, via mechanisms 1 and 2, is essential. We hypothesised that while
217 mechanism 3 cannot compensate for the loss of mechanisms 1 and 2 at native
218 expression levels of RetS, it may be able to compensate at higher expression levels.
219 To test this, we overexpressed RetS(T428A,HDA), which possesses only
220 mechanism 3, in the Δ*retS* mutant. Successful complementation was seen (Fig. 4c)
221 indicating that, at non-physiologically high expression levels, mechanism 3
222 compensates for the loss of mechanisms 1 and 2. However, at physiological
223 expression levels of RetS, this compensation cannot occur, and mechanisms 1 and
224 2 are both required.

225 **Mechanisms 1 and 2 are required for virulence in mice.** We used a mouse model
226 of acute respiratory infection to probe the role of the mechanisms in virulence. Mice
227 were inoculated intranasally with 2 x 10^7 CFUs of *P. aeruginosa*. Only 10% of mice
228 infected with PAO1 survived beyond 28 hours of infection. All mice infected with the
229 Δ*retS* mutant or the mutant lacking mechanism 1 (*retS*(HDA)) survived for the seven-
230 day duration of the experiment, demonstrating that RetS and mechanism 1 are
231 essential for virulence (Fig. 5). The *retS*(T428A) mutant, which lacks mechanism 2,

232 was also severely attenuated in virulence with 80% of mice surviving to the endpoint
233 of the experiment (Fig. 5). These results indicate that mechanisms 1 and 2 are both
234 important for acute virulence.

Discussion

We have shown that two SKs, RetS and GacS, which play a major role in controlling virulence in *P. aeruginosa*, interact extensively, with RetS having three distinct mechanisms for downregulating GacS signalling (Fig. 6). In mechanism 1, RetS takes phosphoryl groups from GacS-P, with phosphotransfer occurring from the autophosphorylation site of GacS to REC2 of RetS. In mechanism 2, RetS has transmitter phosphatase activity that speeds up the dephosphorylation of the REC domain of GacS-P. In mechanism 3, RetS inhibits the autophosphorylation of GacS. These three mechanisms allow RetS to have exquisite control of GacS signalling and they all play significant roles *in vivo* and during infection. In particular, we show that mechanisms 1 and 2 play vital roles during acute respiratory infection in mice. This is the first discovery of such an intricate level of interconnectedness and communication between a pair of SKs in a sensory network. This has profound implications for other sensory networks employing multiple SKs which, in light of this study, could be expected to use similar mechanisms of communication to process sensory data and integrate multiple signals. A further implication is that because of the increased number of different mechanisms by which kinase-to-kinase signalling can occur, multikinase networks may be even more widespread than previously appreciated.

The three mechanisms identified here represent an unprecedented level of communication between two SKs and there is great potential for them to be employed in other multikinase networks. Mechanism 1 employs intermolecular phosphotransfer to signal from the HisKA domain of one SK (GacS) to a REC domain located within another SK (RetS). Here, REC2 of RetS functions as a phosphate sink for GacS. As around 20% of SKs have a REC domain (i.e. are

hybrid/unorthodox), related phosphotransfer mechanisms will be found connecting many other pairs of kinases that work together[12,13,18,46]. Mechanism 2 uses the transmitter phosphatase activity of one SK (RetS) against the REC domain of another SK (GacS); as far as we are aware, this is the first demonstration of transmitter phosphatase activity occurring between two kinases but there is wide potential for it to be employed in other multikinase-networks because almost all SKs have transmitter phosphatase activity[20]. Mechanism 3 involves inhibitory interactions between the catalytic core of two kinases (RetS and GacS)[10], and consistent with this mechanism being used by other networks are the findings of a systematic two-hybrid screen of the SKs from *Myxococcus xanthus*, which tested 725 possible catalytic core/catalytic core interactions and found evidence of interaction in over 100 cases[16].

Mechanism 1 depends on the phosphorylatable aspartate residue in REC2 of RetS (D858) and is essential for virulence, biofilm formation, swarming and normal expression levels of RsmY&Z. Most strikingly, the *retS*(HDA) mutant, lacking D858, was completely avirulent in mice (Fig. 5). Prior to our discovery of its key role in mechanism 1, the role of D858 had been investigated. Similar to our findings with the PAO1 strain of *P. aeruginosa*, Laskowski and Kazmierczak found that for the PA103 strain, D858 is essential for RetS function[56]. However, in contrast, Goodman et al., found no phenotype for the D858 mutation in the PAK strain[10]. This suggests that either of the two remaining mechanisms (which are independent of D858) compensate when mechanism 1 is lost in the PAK strain but not in the PAO1 and PA103 strains.

The three mechanisms that we have demonstrated signal via GacS to control phosphorylation levels of the output RR, GacA, which controls expression of the

285 regulatory RNAs, RsmY and RsmZ. Loss of any individual mechanism is sufficient to
286 increase RsmY expression levels to the same extent as seen in the Δ*retS* mutant
287 (Fig. 2b), whereas although significant elevation in RsmZ levels is seen when
288 individual mechanisms are lost, it is not to the same extent as seen with the Δ*retS*
289 mutant (Fig. 2c). RsmY expression has previously been reported to be at least 2-fold
290 higher than RsmZ expression[55,58]. These findings can be explained by a model
291 where GacA-P binds more tightly to the RsmY promoter than to the RsmZ promoter.
292 Deleting *retS*, eliminates all three of our mechanisms, thereby giving a large rise in
293 GacA-P levels, sufficient to fully activate RsmY and RsmZ expression. The *retS* point
294 mutations, by disabling individual mechanisms, would generate a rise in GacA-P
295 levels but not as much as is seen in the *retS* deletion mutant. This lesser rise in
296 GacA-P levels would be enough to fully activate the RsmY promoter (due to its
297 higher binding affinity) but not enough to fully activate the RsmZ promoter.

298 An intriguing question is why are multiple mechanisms necessary to
299 orchestrate this virulence switch? Presumably, each mechanism contributes uniquely
300 to the balance of the decision-making process during infection and the complexity of
301 this process reflects the importance of the decision to bacterial survival in the host.
302 Differential regulation of the three mechanisms would allow precise control of GacS
303 signalling and, given their importance for virulence, it is tempting to speculate that
304 these elaborate mechanisms constitute a logic gate for processing and integrating
305 the different stimuli sensed by GacS and RetS to decide the course of the infection.
306 Although all three mechanisms allow RetS to downregulate GacS signalling, there
307 are significant differences. For example, mechanism 3 blocks the
308 autophosphorylation of GacS but it differs from mechanisms 1 & 2, as it is unable to
309 dephosphorylate GacS-P. This is important because autophosphorylation is not the

only way of generating GacS-P, as LadS-P phosphorylates GacS[46]; GacS-P generated from LadS-P would be unaffected by mechanism 3 but could be targeted by mechanisms 1 and 2.

How might the three different mechanisms be controlled? RetS has a periplasmic ligand binding domain that has been implicated in detecting kin-cell lysis but its ligand is currently unknown[50,59,60]. Ligand binding could regulate any of the three mechanisms, but in other SKs there is a strong precedent for it regulating the balance between kinase activity and transmitter phosphatase activity[20]. RetS lacks kinase activity but, following this precedent, transmitter phosphatase activity (mechanism 2) is very likely to be under ligand control. Mechanism 1 provides considerable potential for linkage to other signalling pathways, in particular the HptB signalling pathway. HptB is a single domain Hpt protein that relays phosphoryl groups from several hybrid kinases (PA1611, ErcS' and SagS) to the output RR, HsbR, which indirectly controls motility and cyclic-di-GMP levels[54,61,62]. Analogous to how RetS serves as a phosphoacceptor for GacS-P in mechanism 1, RetS can also take phosphoryl groups from HptB-P[61]. This could provide a route for HptB signalling to downregulate mechanism 1, since when RetS is phosphorylated by HptB-P, then, until it has dephosphorylated, it will be unable to accept phosphoryl groups from GacS-P. This potential communication route would expand the number of SKs, and therefore the number of different signals, that could influence signalling by the GacS network. Aside from this HptB mediated link, PA1611 has been shown to interact directly with RetS[51,52]. In wild-type cells, PA1611 is expressed only at very low levels making the physiological relevance of this interaction uncertain[51], however it has been found that overexpression of PA1611 using a multicopy plasmid expression vector, favours the interaction between PA1611 and RetS, and relieves GacS from

335 the inhibitory effects of RetS, suggesting that PA1611 sequesters RetS away from
336 GacS[51]. The phenotypic data from PA1611 overexpression are consistent with a total
337 loss of RetS function[51,52], suggesting that the sequestration of RetS by PA1611
338 blocks all three of the mechanisms by which RetS targets GacS.

339 In conclusion, we have discovered extensive interactions between the GacS
340 and RetS SKs that play a critical role in controlling the switch between acute and
341 chronic infection. We have identified three distinct biochemical mechanisms and
342 demonstrated their important roles *in vivo* and in insect and mouse infection models.
343 The complexity of these mechanisms reflects the importance of the finely balanced
344 decisions that the GacS network makes during infection. As these mechanisms
345 involve highly conserved domains or sequence motifs, they are likely to be used by
346 many other multikinase networks for signal integration and decision-making.

Methods

Bacterial strains and growth conditions. Bacterial strains and plasmids are described in Supplementary Table 1. Unless otherwise stated bacteria were grown in LB broth at 37 °C. When used, M63 (2 g/L $(NH_4)_2SO_4$, 13.6 g/L KH_2PO_4, and 0.5 mg/L $FeSO_4$) was supplemented with 1 mM $MgSO_4$, 0.5 % Casamino Acids and 0.2 % glucose. Antibiotics were used at the following concentrations: ampicillin 100 µg/ml, kanamycin 25 µg/ml, tetracycline 50 µg/ml and gentamycin 25 µg/ml (*E. coli*) or 100 µg/ml (*P. aeruginosa*).

Plasmid construction. Genes for overexpressing wild-type cytoplasmic portions of proteins were amplified from *P. aeruginosa* PAO1 genomic DNA using primers described in Supplementary Table 2. Point mutations were introduced using overlap extension PCR. Wild-type genes and their mutant derivatives were cloned into the pQE60 expression plasmid which attaches a C-terminal 6xHis tag. The proteins were overexpressed and purified as previously described for other SKs[63,64]. Allelic exchange plasmids for in-frame deletion of genes in PAO1 or for introducing point mutations were constructed using primers described in Supplementary Table 2 using *P. aeruginosa* DNA as template. These constructs were cloned into pEX19Gm for allelic exchange with PAO1[65,66].

Strain construction. In-frame gene deletions and allelic exchange of gene regions containing introduced point mutations were carried out by tri-parental mating using *E. coli* containing the mobilisation plasmid, pRK2013[67]. Subsequent sucrose and gentamycin susceptibility tests were done to isolate potential mutants. Deletion mutants were checked via PCR using primers outside of the initial construct used to make the deletion. PCR products were sequenced to confirm mutations. Tetra-primer PCR[68] was used as a preliminary screen to identify strains containing desired

point mutations. Potential mutants were then checked by sequencing using PCR products obtained using primers outside of the original mutation construct.

Autophosphorylation assays. Reactions were performed in TGMNKD buffer (10% (v/v) Glycerol, 150 mM NaCl, 50 mM Tris HCl, 1 mM DTT, 5 mM $MgCl_2$, 50 mM KCl, pH 8.0) and initiated by addition of 2 mM [γ^{32}P] ATP (3.7 GBq/mmol PerkinElmer). The reactions contained 5 μM GacS derivative and 20 μM RetS derivative (Fig. 1m-n). The final reaction volume was 100 μl. 10 μl aliquots were taken at the indicated timepoints and quenched in 20 μl of 2x SDS loading dye (7.5% (w/v) SDS, 90 mM EDTA, 37.5 mM Tris pH 6.8, 37.5% Glycerol, and 3% β-mercaptoethanol). Samples were stored on ice and then analysed using SDS-PAGE (10% (w/v) polyacrylamide). Gels were exposed to phosphorscreens (Fuji) for 1 hour and then analysed using a Fujifilm FLA-7000 phosphorimager. The uncropped phosphorimages used to produce Fig. 1 and Supplementary Fig. 1 are shown in Supplementary Fig. 5&6.

Pre-phosphorylation of GacS derivatives. GacSc, GacSc(HAQ) and GacSc(HDQ) were purified and then incubated with 2 mM [γ^{32}P] ATP (3.7 GBq/mmol PerkinElmer) for 1 hour at 20 °C. The phosphorylated proteins were then diluted in lysis buffer and purified away from unincorporated ATP using a Ni-NTA column[69,70].

GacS-P dephosphorylation assays. Reaction tubes contained TGMNKD buffer and, where appropriate, RetSc or one of its mutant derivatives. The reactions were initiated by addition of phosphorylated GacS (either wild-type GacSc-P or one of its mutant derivatives). Reactions contained: 2 μM GacSc-P and 50 μM RetSc derivative (Fig. 1a-d and Supplementary Fig. 1a-c), 4 μM GacSc(HAQ)-P and 20 μM RetSc derivative (Fig. 1e-h and Supplementary Fig. 1d-f), 2 μM GacSc-P and 20 μM RetSc derivative (Fig. 1j,k), and 2 μM GacSc(HDQ)-P and 20 μM RetSc derivative (Supplementary Fig. 2). Reactions were performed at 20 ^{o}C. 10 μl samples were

taken at the timepoints indicated and processed as described for the autophosphorylation assays. Half-times of GacSc-P dephosphorylation were calculated using Origin 4.1. Data were analysed using a One-Way ANOVA with Tukey's modification.

Biofilm formation. Biofilm formation was measured using the MBEC^{TM} (Minimum Biofilm Eradication Concentration) Assay from Innovotech. This features a 96-well plate with a peg lid and was used according to a modified method previously described[71]. Overnight LB cultures were standardised in LB broth to an OD_{600nm}=1.0, which were then diluted 1:100 in M63. In each well, 150 µl of diluted culture or uninoculated broth was dispensed before the sterile peg lid was sealed on the plate. Each strain had 5 technical repeats per plate. The plates were incubated for 10 hrs at 37 °C with shaking at 125 rpm. Peg lids were removed and washed in PBS before being dried at 65 °C. Dried lids were stained with 0.1% (w/v) crystal violet. The pegs were washed 3 times in PBS, 5 minutes per wash, before bound crystal violet was solubilised in 95% ethanol. These plates were read at OD_{570nm}. Three biological repeats were performed.

RNA extraction, cDNA and qPCR. Overnight cultures were subcultured into LB broth with a starting OD_{600nm} of 0.03 and incubated for 6 hrs at 37 °C with shaking. Cells were harvested and processed following the supplier's protocol through the RiboPure Bacteria Kit (Ambion), which includes a DNA removal step, which was repeated twice. Purified RNA was checked by PCR for DNA contamination before cDNA was made using SuperScript III reverse Transcriptase (Life Technologies) following the supplier's protocol. Quantitative real time PCR (qRT-PCR) was carried out on a Stratagene Mx3005P machine using Brilliant III Ultra-Fast SYBR Green qPCR kit (Agilent Technologies) following the manufacturer's protocol. The

oligonucleotides used are detailed in Supplementary Table 2. The housekeeping gene *rpoC* was used an internal control. Fold changes in expression were calculated using the $2^{-\Delta\Delta C_T}$ method[72]. Data were analysed using a one-way ANOVA with contrasts.

Swarming motility assay. Large swarming plates (140 mm) contained 0.5% (w/v) agar (LAB Agar No2 Bacteriological) and 8 g/L nutrient broth (Oxoid) supplemented with 0.5% (w/v) glucose. Plates were inoculated with 0.5 µl overnight culture, incubated at 20 °C for 2 hrs prior to incubation at 30 °C for 16 hrs. Plates were then incubated at 20 °C for a further 8 hours before imaging.

***Galleria mellonella* infection model.** *Galleria* larvae killing was performed based on a previously described assay[73]. *Galleria* larvae were obtained from UK Waxworms Ltd (Sheffield, UK). *P. aeruginosa* stains were grown overnight in M63 before being centrifuged, washed and resuspended in PBS to an OD_{590}=1 ± 0.05. This was diluted 5 x 10^5 fold in PBS. Using a gastight repeat dispenser Hamilton syringe, 2 X 5 µl of the diluted bacterial suspension (20-40 CFUs) were injected into the hindmost proleg of the larvae. Larvae were incubated at 37 °C and their survival was monitored after 15 hours of incubation for up to 47 hours. Data were analysed using Kaplan-Meier survival curves. Statistical significance was assessed using the Mantel-Cox Log Rank test, applying Bonferroni's correction for multiple comparisons.

Mouse respiratory infection model. The mouse infection model was done as previously described[74]. 7-9 week old female Balb/c mice (Harlan) were anesthetized with O_2 and isoflurane and infected intranasally with a challenge dose of $2x10^7$ CFUs. Two independent experiments were performed, each with five mice per strain. Power calculations were used to estimate the number of mice needed to detect a 10 % change in the mean survival time. Mice were randomly assigned to each of the

447 treatment groups. No blinding was used. Survival was followed over 7 days and
448 scored as previously described[74]. Mouse experiments were approved by the United
449 Kingdom Home Office (Home Office Project License Number 40/3602) and the
450 University of Liverpool Animal Welfare and Ethics Committee.

451 **Western Blot.** Overnight LB cultures were standardised in LB broth to an
452 OD_{600nm}=1.0, which were then diluted 1:100 in M63. Cells were incubated for 10 hrs
453 at 37 °C with shaking at 125 rpm. 1 ml of cells was centrifuged at 13,000 rpm. Cell
454 pellets were resuspended in 100 µl of BugBuster (Merck) and incubated at 20 °C for
455 20 minutes to lyse cells. 25 µl NuPAGE® LDS sample buffer (4X) (Invitrogen) was
456 added and samples were boiled for 5 minutes at 100 °C. Whole cell lysates were
457 separated using Bis-Tris NuPAGE® Novex® 4 to 12% SDS-PAGE gels (Invitrogen).
458 Proteins were electrically transferred to a nitrocellulose membrane (Fisher) and
459 blocked overnight at 4 °C using 3% (w/v) skimmed milk (Sigma) in TPBS (PBS
460 supplemented with 1% (v/v) Tween-20). The membrane was incubated at 20 °C for
461 30 mins before being incubated for 90 minutes with 3% (w/v) skimmed milk in TPBS
462 with the primary antibody (rabbit) diluted 1:1000. The primary rabbit antibody was
463 raised against the purified cytoplasmic portion of RetS (Eurogentec). The membrane
464 was washed three times for 5 minutes in TPBS. It was then incubated for 90 minutes
465 with a secondary antibody (goat anti-rabbit) with an infrared dye (IRDye® 800W
466 secondary antibodies from *Li-Cor*) diluted 1:25000 in TPBS with 3% (w/v) skimmed
467 milk. The membrane was washed three times for 5 minutes with TPBS and imaged
468 on the *Li-Cor* Odyssey.

469 **Data availability**

470 The authors declare that the data supporting the findings of this study are available
471 within the paper and its supplementary information files.

References

1. Stock, A.M., Robinson, V.L. & Goudreau, P.N. Two-component signal transduction. *Annu. Rev. Biochem.* **69**, 183-215 (2000).
2. Skerker, J.M., Prasol, M.S., Perchuk, B.S., Biondi, E.G. & Laub, M.T. Two-component signal transduction pathways regulating growth and cell cycle progression in a bacterium: a system-level analysis. *PLoS Biol.* **3**, e334 (2005).
3. Kirkpatrick, C.L. & Viollier, P.H. Decoding *Caulobacter* development. *FEMS Microbiol. Rev.* **36**, 193-205 (2012).
4. Tsokos, C.G., Perchuk, B.S. & Laub, M.T. A dynamic complex of signaling proteins uses polar localization to regulate cell-fate asymmetry in *Caulobacter crescentus*. *Dev. Cell* **20**, 329-341 (2011).
5. Childers, W.S. et al. Cell fate regulation governed by a repurposed bacterial histidine kinase. *PLoS Biol.* **12**, e1001979 (2014).
6. Jiang, M., Shao, W., Perego, M. & Hoch, J.A. Multiple histidine kinases regulate entry into stationary phase and sporulation in *Bacillus subtilis*. *Mol. Microbiol.* **38**, 535-542 (2000).
7. Porter, S.L., Wadhams, G.H. & Armitage, J.P. Signal processing in complex chemotaxis pathways. *Nat. Rev. Microbiol.* **9**, 153-165 (2011).
8. Drepper, T. et al. Cross-talk towards the response regulator NtrC controlling nitrogen metabolism in *Rhodobacter capsulatus*. *FEMS Microbiol. Lett.* **258**, 250-256 (2006).
9. Mike, L.A. et al. Two-component system cross-regulation integrates *Bacillus anthracis* response to heme and cell envelope stress. *PLoS Pathog.* **10**, e1004044 (2014).
10. Goodman, A.L. et al. Direct interaction between sensor kinase proteins mediates acute and chronic disease phenotypes in a bacterial pathogen. *Genes Dev.* **23**, 249-259 (2009).
11. Ng, W.L. & Bassler, B.L. Bacterial quorum-sensing network architectures. *Annu. Rev. Genet.* **43**, 197-222 (2009).
12. Mikkelsen, H., Hui, K., Barraud, N. & Filloux, A. The pathogenicity island encoded PvrSR/RcsCB regulatory network controls biofilm formation and dispersal in *Pseudomonas aeruginosa* PA14. *Mol. Microbiol.* **89**, 450-463 (2013).
13. Schramm, A., Lee, B. & Higgs, P.I. Intra- and inter-protein phosphorylation between two hybrid histidine kinases controls *Myxococcus xanthus* developmental progression. *J. Biol. Chem.* **287**, 25060-25072 (2012).
14. Higgs, P.I., Cho, K.Y., Whitworth, D.E., Evans, L.S. & Zusman, D.R. Four unusual two-component signal transduction homologs, RedC to RedF, are necessary for timely development in *Myxococcus xanthus*. *J. Bacteriol.* **187**, 8191-8195 (2005).
15. Willett, J.W. & Crosson, S. Atypical modes of bacterial histidine kinase signaling. *Mol. Microbiol.* **103**, 197-202 (2017).
16. Whitworth, D.E., Millard, A., Hodgson, D.A. & Hawkins, P.F. Protein-protein interactions between two-component system transmitter and receiver domains of *Myxococcus xanthus*. *Proteomics* **8**, 1839-1842 (2008).
17. Francis, V.I., Stevenson, E.C. & Porter, S.L. Two-component systems required for virulence in *Pseudomonas aeruginosa*. *FEMS Microbiol. Lett.* **364**, fnx104 (2017).
18. Wuichet, K., Cantwell, B.J. & Zhulin, I.B. Evolution and phyletic distribution of two-component signal transduction systems. *Curr. Opin. Microbiol.* **13**, 219-225 (2010).
19. Galperin, M.Y. Structural classification of bacterial response regulators: diversity of output domains and domain combinations. *J. Bacteriol.* **188**, 4169-4182 (2006).
20. Huynh, T.N. & Stewart, V. Negative control in two-component signal transduction by transmitter phosphatase activity. *Mol. Microbiol.* **82**, 275-286 (2011).
21. Silversmith, R.E. Auxiliary phosphatases in two-component signal transduction. *Curr. Opin. Microbiol.* **13**, 177-183 (2010).

22. Dutta, R., Yoshida, T. & Inouye, M. The critical role of the conserved Thr247 residue in the functioning of the osmosensor EnvZ, a histidine kinase/phosphatase, in *Escherichia coli*. *J. Biol. Chem.* **275**, 38645-38653 (2000).
23. Skerker, J.M. et al. Rewiring the specificity of two-component signal transduction systems. *Cell* **133**, 1043-1054 (2008).
24. Podgornaia, A.I. & Laub, M.T. Determinants of specificity in two-component signal transduction. *Curr. Opin. Microbiol.* **16**, 156-162 (2013).
25. Willett, J.W. et al. Specificity residues determine binding affinity for two-component signal transduction systems. *mBio* **4**, e00420-13 (2013).
26. Kenney, L.J. How important is the phosphatase activity of sensor kinases? *Curr. Opin. Microbiol.* **13**, 168-176 (2010).
27. Siryaporn, A. & Goulian, M. Characterizing cross-talk *in vivo*: avoiding pitfalls and overinterpretation. *Methods Enzymol.* **471**, 1-16 (2010).
28. Laub, M.T. & Goulian, M. Specificity in two-component signal transduction pathways. *Annu. Rev. Genet.* **41**, 121-145 (2007).
29. Capra, E.J., Perchuk, B.S., Skerker, J.M. & Laub, M.T. Adaptive mutations that prevent crosstalk enable the expansion of paralogous signaling protein families. *Cell* **150**, 222-232 (2012).
30. Brewer, S.C., Wunderink, R.G., Jones, C.B. & Leeper, K.V., Jr. Ventilator-associated pneumonia due to *Pseudomonas aeruginosa*. *Chest* **109**, 1019-1029 (1996).
31. Pendleton, J.N., Gorman, S.P. & Gilmore, B.F. Clinical relevance of the ESKAPE pathogens. *Expert Rev. Anti Infect. Ther.* **11**, 297-308 (2013).
32. Furukawa, S., Kuchma, S.L. & O'Toole, G.A. Keeping their options open: acute versus persistent infections. *J. Bacteriol.* **188**, 1211-1217 (2006).
33. Costerton, J.W., Stewart, P.S. & Greenberg, E.P. Bacterial biofilms: a common cause of persistent infections. *Science* **284**, 1318-1322 (1999).
34. Valentini, M., Gonzalez, D., Mavridou, D.A.I. & Filloux, A. Lifestyle transitions and adaptive pathogenesis of *Pseudomonas aeruginosa*. *Curr. Opin. Microbiol.* **41**, 15-20 (2018).
35. Lapouge, K., Schubert, M., Allain, F.H. & Haas, D. Gac/Rsm signal transduction pathway of γ-proteobacteria: from RNA recognition to regulation of social behaviour. *Mol. Microbiol.* **67**, 241-253 (2008).
36. Coggan, K.A. & Wolfgang, M.C. Global regulatory pathways and cross-talk control *Pseudomonas aeruginosa* environmental lifestyle and virulence phenotype. *Curr. Issues Mol. Biol.* **14**, 47-69 (2012).
37. Raghavan, V. & Groisman, E.A. Orphan and hybrid two-component system proteins in health and disease. *Curr. Opin. Microbiol.* **13**, 226-231 (2010).
38. Balasubramanian, D., Schneper, L., Kumari, H. & Mathee, K. A dynamic and intricate regulatory network determines *Pseudomonas aeruginosa* virulence. *Nucleic Acids Res.* **41**, 1-20 (2013).
39. Pessi, G. et al. The global posttranscriptional regulator RsmA modulates production of virulence determinants and N-Acylhomoserine lactones in *Pseudomonas aeruginosa*. *J. Bacteriol.* **183**, 6676-6683 (2001).
40. Heurlier, K. et al. Positive control of swarming, rhamnolipid synthesis, and lipase production by the posttranscriptional RsmA/RsmZ system in *Pseudomonas aeruginosa* PAO1. *J. Bacteriol.* **186**, 2936-2945 (2004).
41. Burrowes, E., Baysse, C., Adams, C. & O'Gara, F. Influence of the regulatory protein RsmA on cellular functions in *Pseudomonas aeruginosa* PAO1, as revealed by transcriptome analysis. *Microbiology* **152**, 405-418 (2006).
42. Gooderham, W.J. & Hancock, R.E.W. Regulation of virulence and antibiotic resistance by two-component regulatory systems in *Pseudomonas aeruginosa*. *FEMS Microbiol. Rev.* **33**, 279-294 (2009).

43. Allsopp, L.P. et al. RsmA and AmrZ orchestrate the assembly of all three type VI secretion systems in *Pseudomonas aeruginosa*. *Proc. Natl. Acad. Sci. USA* **114**, 7707-7712 (2017).
44. Broder, U.N., Jaeger, T. & Jenal, U. LadS is a calcium-responsive kinase that induces acute-to-chronic virulence switch in *Pseudomonas aeruginosa*. *Nat. Microbiol.* **2**, 16184 (2016).
45. Ventre, I. et al. Multiple sensors control reciprocal expression of *Pseudomonas aeruginosa* regulatory RNA and virulence genes. *Proc. Natl. Acad. Sci. USA* **103**, 171-176 (2006).
46. Chambonnier, G. et al. The hybrid histidine kinase LadS Forms a multicomponent signal transduction system with the GacS/GacA two-component system in *Pseudomonas aeruginosa*. *PLoS Genet.* **12**, e1006032 (2016).
47. Goodman, A.L. et al. A signaling network reciprocally regulates genes associated with acute infection and chronic persistence in *Pseudomonas aeruginosa*. *Dev. Cell* **7**, 745-754 (2004).
48. Laskowski, M.A., Osborn, E. & Kazmierczak, B.I. A novel sensor kinase–response regulator hybrid regulates type III secretion and is required for virulence in *Pseudomonas aeruginosa*. *Mol. Microbiol.* **54**, 1090-1103 (2004).
49. Workentine, M.L., Chang, L., Ceri, H. & Turner, R.J. The GacS-GacA two-component regulatory system of *Pseudomonas fluorescens*: a bacterial two-hybrid analysis. *FEMS Microbiol. Lett.* **292**, 50-56 (2009).
50. LeRoux, M. et al. Kin cell lysis is a danger signal that activates antibacterial pathways of *Pseudomonas aeruginosa*. *eLife* **4**, e05701 (2015).
51. Kong, W. et al. Hybrid sensor kinase PA1611 in *Pseudomonas aeruginosa* regulates transitions between acute and chronic infection through direct interaction with RetS. *Mol. Microbiol.* **88**, 784-797 (2013).
52. Bhagirath, A.Y. et al. Characterization of the direct interaction between hybrid sensor kinases PA1611 and RetS that controls biofilm formation and the type III secretion system in *Pseudomonas aeruginosa*. *ACS Infect. Dis.* **3**, 162-175 (2017).
53. Willett, J.W. & Kirby, J.R. Genetic and biochemical dissection of a HisKA domain identifies residues required exclusively for kinase and phosphatase activities. *PLoS Genet.* **8**, e1003084 (2012).
54. Bordi, C. et al. Regulatory RNAs and the HptB/RetS signalling pathways fine-tune *Pseudomonas aeruginosa* pathogenesis. *Mol. Microbiol.* **76**, 1427-1443 (2010).
55. Brencic, A. et al. The GacS/GacA signal transduction system of *Pseudomonas aeruginosa* acts exclusively through its control over the transcription of the RsmY and RsmZ regulatory small RNAs. *Mol. Microbiol.* **73**, 434-445 (2009).
56. Laskowski, M.A. & Kazmierczak, B.I. Mutational analysis of RetS, an unusual sensor kinase-response regulator hybrid required for *Pseudomonas aeruginosa* virulence. *Infect. Immun.* **74**, 4462-4473 (2006).
57. Grocock, R.J. & Sharp, P.M. Synonymous codon usage in *Pseudomonas aeruginosa* PA01. *Gene* **289**, 131-139 (2002).
58. Kay, E. et al. Two GacA-dependent small RNAs modulate the quorum-sensing response in *Pseudomonas aeruginosa*. *J. Bacteriol.* **188**, 6026-6033 (2006).
59. Jing, X., Jaw, J., Robinson, H.H. & Schubot, F.D. Crystal structure and oligomeric state of the RetS signaling kinase sensory domain. *Proteins* **78**, 1631-1640 (2010).
60. Vincent, F. et al. Distinct oligomeric forms of the *Pseudomonas aeruginosa* RetS sensor domain modulate accessibility to the ligand binding site. *Environ. Microbiol.* **12**, 1775-1786 (2010).
61. Hsu, J.L., Chen, H.C., Peng, H.L. & Chang, H.Y. Characterization of the histidine-containing phosphotransfer protein B-mediated multistep phosphorelay system in *Pseudomonas aeruginosa* PAO1. *J. Biol. Chem.* **283**, 9933-9944 (2008).
62. Valentini, M., Laventie, B.-J., Moscoso, J., Jenal, U. & Filloux, A. The diguanylate cyclase HsbD intersects with the HptB regulatory cascade to control *Pseudomonas aeruginosa* biofilm and motility. *PLoS Genet.* **12**, e1006354 (2016).

63. Porter, S.L., Wadhams, G.H. & Armitage, J.P. *In vivo* and *in vitro* analysis of the *Rhodobacter sphaeroides* chemotaxis signaling complexes. *Methods Enzymol.* **423**, 392-413 (2007).
64. Scott, K.A. et al. Specificity of localization and phosphotransfer in the CheA proteins of *Rhodobacter sphaeroides*. *Mol. Microbiol.* **76**, 318-330 (2010).
65. Hoang, T.T., Karkhoff-Schweizer, R.R., Kutchma, A.J. & Schweizer, H.P. A broad-host-range Flp-FRT recombination system for site-specific excision of chromosomally-located DNA sequences: application for isolation of unmarked *Pseudomonas aeruginosa* mutants. *Gene* **212**, 77-86 (1998).
66. Guvener, Z.T. & Harwood, C.S. Subcellular location characteristics of the *Pseudomonas aeruginosa* GGDEF protein, WspR, indicate that it produces cyclic-di-GMP in response to growth on surfaces. *Mol. Microbiol.* **66**, 1459-1473 (2007).
67. Figurski, D.H. & Helinski, D.R. Replication of an origin-containing derivative of plasmid RK2 dependent on a plasmid function provided in trans. *Proc. Natl. Acad. Sci. USA* **76**, 1648-1652 (1979).
68. Ye, S., Dhillon, S., Ke, X., Collins, A.R. & Day, I.N.M. An efficient procedure for genotyping single nucleotide polymorphisms. *Nucleic Acids Res.* **29**, e88-e88 (2001).
69. Amin, M. et al. Phosphate sink containing two-component signaling systems as tunable threshold devices. *PLoS Comput. Biol.* **10**, e1003890 (2014).
70. Amin, M., Porter, S.L. & Soyer, O.S. Split histidine kinases enable ultrasensitivity and bistability in two-component signaling networks. *PLoS Comput. Biol.* **9**, e1002949 (2013).
71. O'Toole, G.A. & Kolter, R. Flagellar and twitching motility are necessary for *Pseudomonas aeruginosa* biofilm development. *Mol. Microbiol.* **30**, 295-304 (1998).
72. Livak, K.J. & Schmittgen, T.D. Analysis of relative gene expression data using real-time quantitative PCR and the $2^{-\Delta\Delta CT}$ method. *Methods* **25**, 402-408 (2001).
73. Seed, K.D. & Dennis, J.J. Development of *Galleria mellonella* as an alternative infection model for the *Burkholderia cepacia* Complex. *Infect. Immun.* **76**, 1267-1275 (2008).
74. Carter, M.E.K. et al. A subtype of a *Pseudomonas aeruginosa* cystic fibrosis epidemic strain exhibits enhanced virulence in a murine model of acute respiratory infection. *J. Infect. Dis.* **202**, 935-942 (2010).

Acknowledgements

This work was supported by the Medical Research Council (MRC) [grant number MR/M020045/1], the Leverhulme Trust [grant number RPG-2014-228], the RoseTrees Trust [grant number M328] and a NERC PhD studentship [grant number 1076449]. We are grateful to Lily Byham, Charlotte Unwin and Adam Wise for their assistance. We would like to thank Alain Filloux for useful discussions.

Author contributions

V.I.F., S.E.F-J, A.G., E.W and S.L.P. conducted the experiments; V.I.F., E.W., A.K., A.R.B. and S.L.P. designed the experiments and wrote the paper.

Competing interests

The authors declare no competing interests.

Figure legends

Figure 1 | RetS downregulates GacS signalling via three distinct mechanisms. **a-i**, Mechanism 1 – RetS takes phosphoryl groups from GacS-P. Phosphorimages of SDS-PAGE gels showing phosphotransfer from (**a-d**) GacSc-P to (**a**) buffer control, (**b**) RetSc, (**c**) RetSc(HDA) and (**d**) RetSc(HAA), and from (**e-h**) GacSc(HAQ)-P to (**e**) buffer control, (**f**) RetSc, (**g**) RetSc(HDA) and (**h**) RetSc(HAA). Experiments were repeated 5 times and a representative image shown. **i**, Cartoon depicting mechanism 1, where phosphotransfer occurs from the His residue in the HisKA domain of GacS to D858 in REC2 of RetS.

j-l, Mechanism 2 - RetS has transmitter phosphatase activity against GacS-P. **j**, Phosphorimages of SDS-PAGE gels measuring the dephosphorylation of GacSc-P alone (*top*) and with $RetS_{HK}$ (*bottom*). **k**, GacS-P dephosphorylation half-times in the presence of various RetS mutant proteins. Error bars show SEM from 8 replicates. * significantly faster than GacSc-P autodephosphorylation ($P < 0.05$, one-way ANOVA). **l**, Cartoon depicting mechanism 2, where RetS uses transmitter phosphatase activity against the REC domain of GacS-P.

m-o, Mechanism 3 - RetS inhibits the GacS autophosphorylation reaction. Phosphorimages of SDS-PAGE gels comparing the autophosphorylation of: (**m**) GacSc(HAQ) on its own (*top*), with RetSc(HAA) (*middle*), and with RetSc(T428A,HDA) (*bottom*). (**n**) $GacS_{HK}$ on its own (*top*) and with $RetS_{HK}$ (*bottom*). Experiments were repeated 8 times and a representative image shown. **o**, Cartoon depicting mechanism 3, where the catalytic core of RetS blocks the autophosphorylation of GacS.

Figure 2 | Mechanisms 1 and 2 control biofilm formation and the expression levels of RsmY, while all three mechanisms contribute to controlling RsmZ

693 **levels. a**, Quantification of biofilm formation on peg-lidded 96-well plate by crystal
694 violet staining. Plates inoculated with the mutant strains were incubated for 10 hrs
695 with shaking at 37 °C. Error bars show SEM (three biological repeats each
696 containing five technical repeats). * indicates significantly different comparisons (P <
697 0.05, one-way ANOVA). See also Supplementary Fig. 4 for these mutations in a
698 Δ*gacS* background. **b**,**c**, Relative expression level of RsmY (**b**) and RsmZ (**c**) in the
699 mutant strains relative to the wild-type PAO1 strain. RNA levels were measured
700 using qRT-PCR. Error bars show SEM (three biological repeats, with 3 technical
701 repeats per biological repeat). * indicates significantly different comparisons (P
702 <0.05, one-way ANOVA). The mechanisms disabled in each mutant strain are
703 indicated.

704 **Figure 3 | Mechanism 1 is required for swarming motility. a-d**, Representative
705 images of the swarming of the wild-type PAO1 strain and its mutant derivatives.
706 Experiments were repeated three times. The mechanisms disabled in each mutant
707 strain are indicated in circles.

708 **Figure 4 | Mechanisms 1 and 2 are important for virulence in *Galleria***
709 ***mellonella*.**
710 **a**, Survival of *G. mellonella* larvae infected with the *retS* mutant strains. * indicates
711 strains showing significantly attenuated virulence compared to PAO1 (P < 0.01,
712 Mantel-Cox Log Rank with Bonferroni's correction for multiple comparisons). **b**, The
713 *retS* point mutations have no phenotype in a Δ*gacS* background. * indicates strains
714 showing significantly attenuated virulence compared to PAO1 (P < 0.01, Mantel-Cox
715 Log Rank with Bonferroni's correction for multiple comparisons). **c**, Complementation
716 of the Δ*retS* mutant by overexpressing RetS(T428A,HDA)**.** * significantly more
717 virulent than the Δ*retS*-pJN105 strain (P < 0.01, Mantel-Cox Log Rank with

718 Bonferroni's correction for multiple comparisons). **a**-**c**, The mechanisms absent from
719 each strain are indicated in grey circles (except in the Δ*gacS* background strains that
720 lack the target of these mechanisms). Three independent experiments were
721 conducted each with 10 larvae per strain (30 larvae in total per mutant). The
722 inoculum was 20-40 CFUs per larvae.

723 **Figure 5 | Mechanisms 1 and 2 are important for virulence in mice.** Survival of
724 mice infected intranasally with the *retS* mutant strains. Mice infected with the wild-
725 type PAO1 strain developed an acute respiratory infection. Two independent
726 experiments were performed, each with 5 mice per mutant strain (10 mice per
727 mutant strain). The inoculum was 2 x 10^7 CFUs per mouse. * indicates strains
728 showing significantly attenuated virulence compared to PAO1 ($P < 0.01$, Mantel-Cox
729 Log Rank with Bonferroni's correction for multiple comparisons). The mechanisms
730 absent from each strain are indicated in grey circles.

731 **Figure 6 | The three mechanisms used by RetS to inhibit GacS signalling.**
732 Mechanism **1** – D858 in REC2 of RetS takes the phosphoryl group from the
733 autophosphorylatable His residue in the HisKA domain of GacS. Mechanism **2** –
734 RetS uses its transmitter phosphatase activity to accelerate the dephosphorylation of
735 the REC domain of GacS-P. Mechanism **3** – The catalytic core of RetS inhibits the
736 GacS autophosphorylation reaction.
737

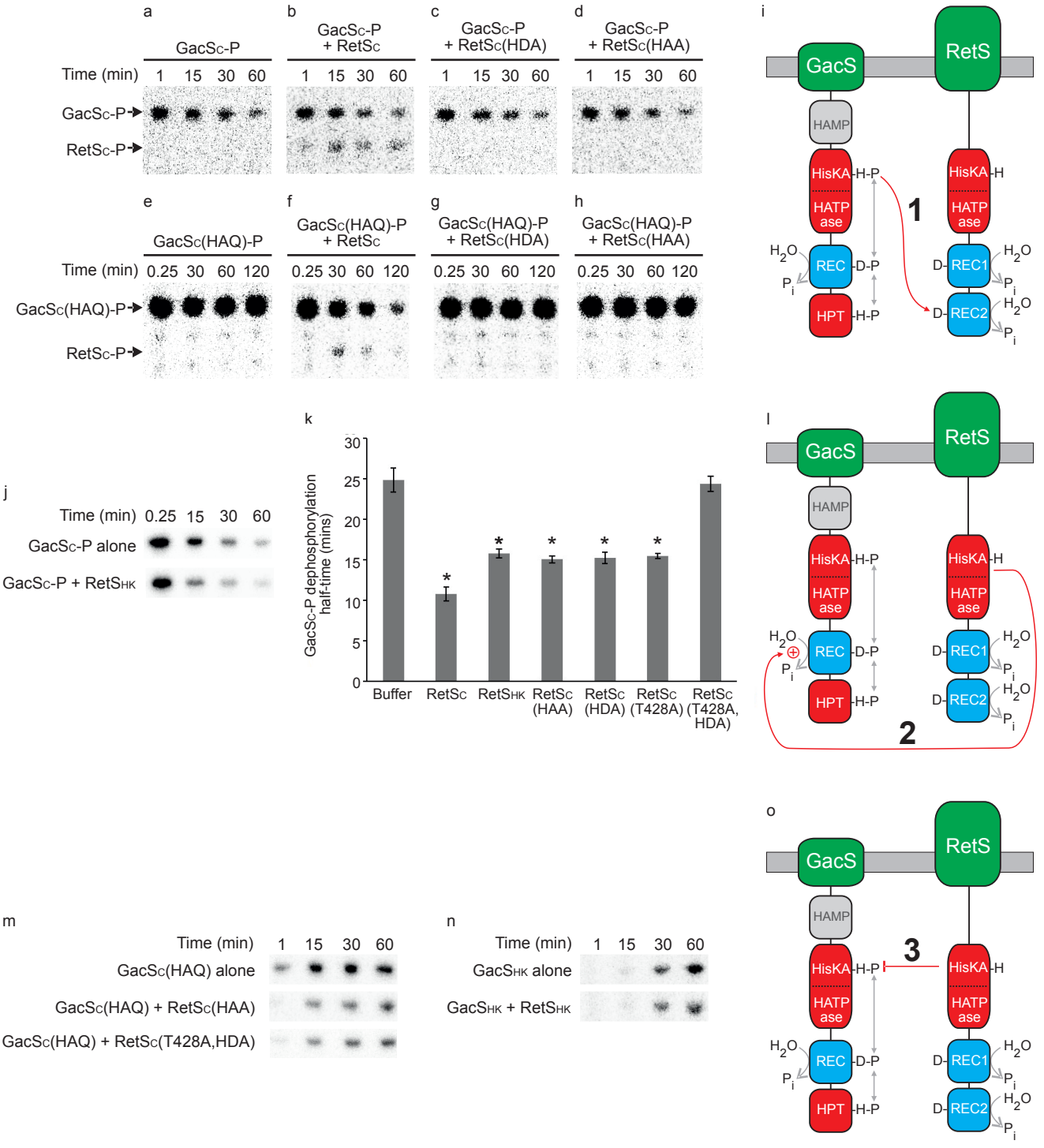
a
GacSc-P
Time (min) 1 15 30 60
GacSc-P
RetSc-P
b
GacSc-P + RetSc
1 15 30 60
c
GacSc-P + RetSc(HDA)
1 15 30 60
d
GacSc-P + RetSc(HAA)
1 15 30 60
e
GacSc(HAQ)-P
Time (min) 0.25 30 60 120
GacSc(HAQ)-P
RetSc-P
f
GacSc(HAQ)-P + RetSc
0.25 30 60 120
g
GacSc(HAQ)-P + RetSc(HDA)
0.25 30 60 120
h
GacSc(HAQ)-P + RetSc(HAA)
0.25 30 60 120
i
GacS
RetS
HAMP
HisKA
HATPase
REC
HPT
REC1
REC2
H-P
D-P
1
l
2
o
3
j
Time (min) 0.25 15 30 60
GacSc-P alone
GacSc-P + RetSHK
k
GacSc-P dephosphorylation half-time (mins)
Buffer
RetSc
RetSHK
RetSc (HAA)
RetSc (HDA)
RetSc (T428A)
RetSc (T428A, HDA)
m
Time (min) 1 15 30 60
GacSc(HAQ) alone
GacSc(HAQ) + RetSc(HAA)
GacSc(HAQ) + RetSc(T428A,HDA)
n
Time (min) 1 15 30 60
GacSHK alone
GacSHK + RetSHK

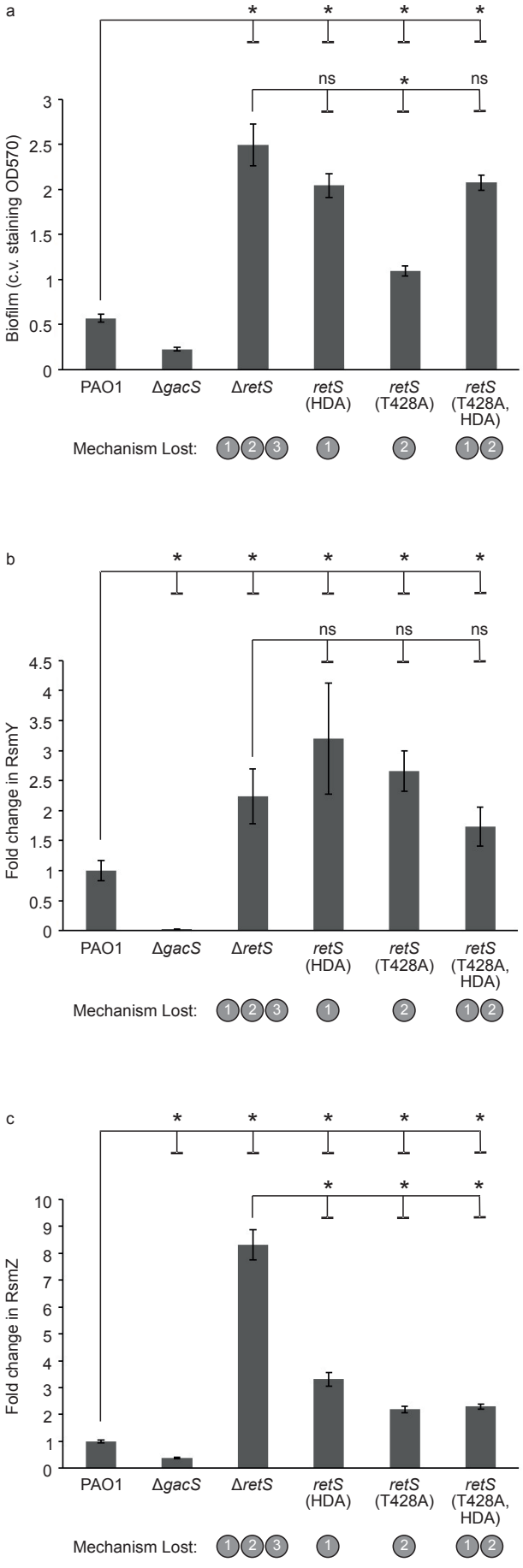
a
Biofilm (c.v. staining OD570)
0
0.5
1
1.5
2
2.5
3
*
*
*
*
ns
*
ns
PAO1
ΔgacS
ΔretS
retS (HDA)
retS (T428A)
retS (T428A, HDA)
Mechanism Lost:
1 2 3
1
2
1 2
b
Fold change in RsmY
0
0.5
1
1.5
2
2.5
3
3.5
4
4.5
*
*
*
*
*
ns
ns
ns
PAO1
ΔgacS
ΔretS
retS (HDA)
retS (T428A)
retS (T428A, HDA)
Mechanism Lost:
1 2 3
1
2
1 2
c
Fold change in RsmZ
0
1
2
3
4
5
6
7
8
9
10
*
*
*
*
*
*
*
*
PAO1
ΔgacS
ΔretS
retS (HDA)
retS (T428A)
retS (T428A, HDA)
Mechanism Lost:
1 2 3
1
2
1 2

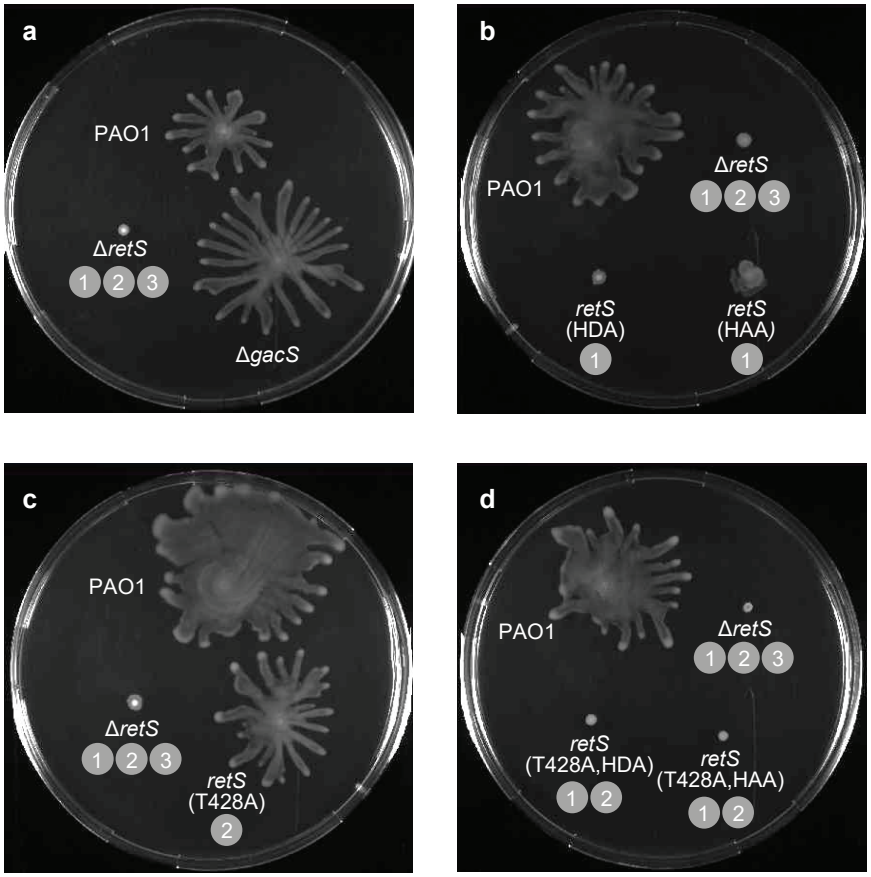
a
PAO1
ΔretS
1 2 3
ΔgacS
b
PAO1
ΔretS
1 2 3
retS
(HDA)
1
retS
(HAA)
1
c
PAO1
ΔretS
1 2 3
retS
(T428A)
2
d
PAO1
ΔretS
1 2 3
retS
(T428A,HDA)
1 2
retS
(T428A,HAA)
1 2

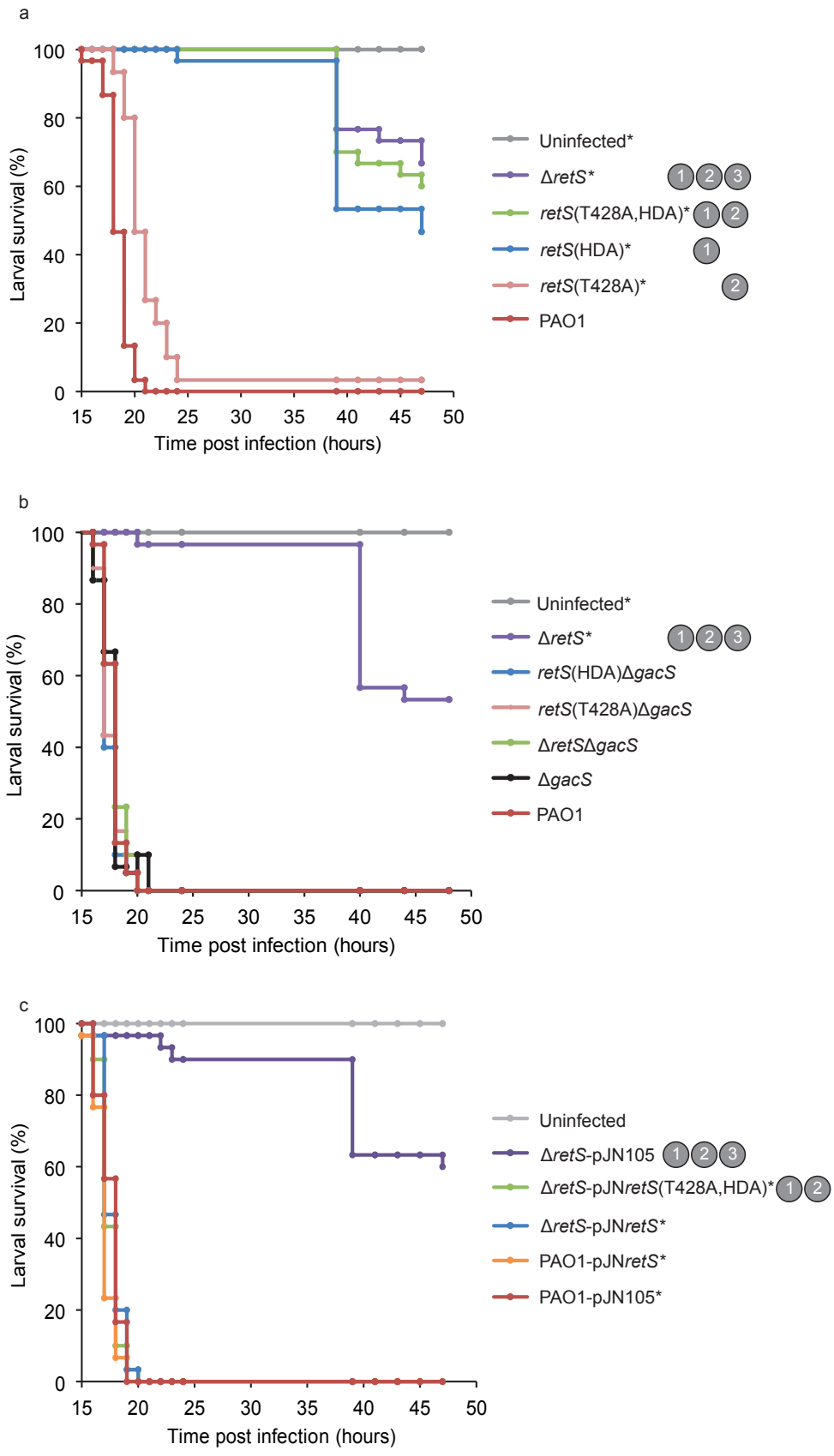
a
Larval survival (%)
Time post infection (hours)
Uninfected*
ΔretS* 1 2 3
retS(T428A,HDA)* 1 2
retS(HDA)* 1
retS(T428A)* 2
PAO1
b
Larval survival (%)
Time post infection (hours)
Uninfected*
ΔretS* 1 2 3
retS(HDA)ΔgacS
retS(T428A)ΔgacS
ΔretSΔgacS
ΔgacS
PAO1
c
Larval survival (%)
Time post infection (hours)
Uninfected
ΔretS-pJN105 1 2 3
ΔretS-pJNretS(T428A,HDA)* 1 2
ΔretS-pJNretS*
PAO1-pJNretS*
PAO1-pJN105*

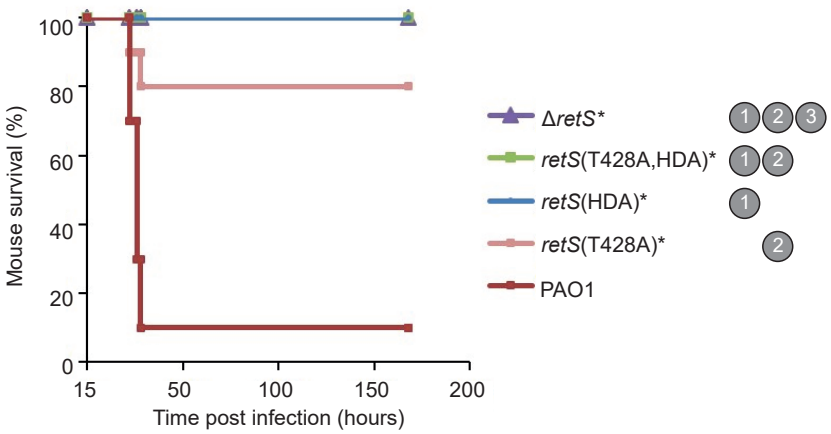
100
80
60
40
20
0
Mouse survival (%)
15
50
100
150
200
Time post infection (hours)
ΔretS*
retS(T428A,HDA)*
retS(HDA)*
retS(T428A)*
PAO1
1 2 3
1 2
1
2

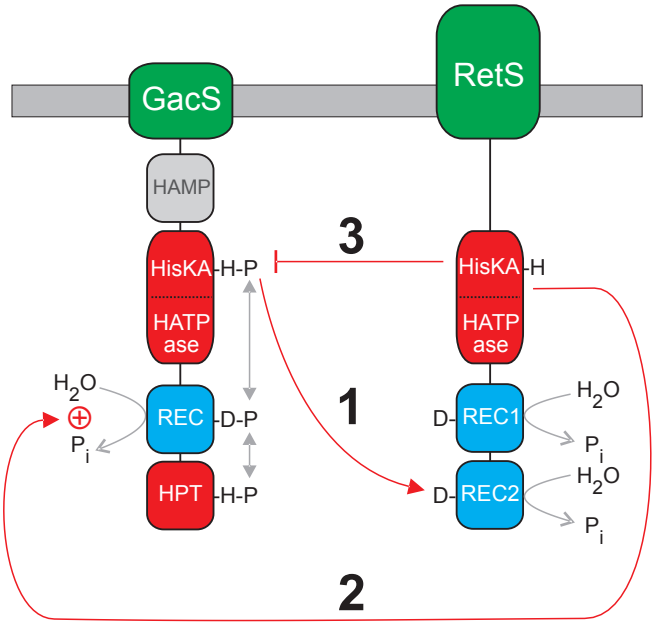
GacS
RetS
HAMP
HisKA
H-P
HATP
ase
REC
D-P
HPT
H-P
HisKA
H
HATP
ase
D-
REC1
D-
REC2
H2O
Pi
H2O
Pi
H2O
Pi
3
1
2